output PSDs for the noisy input case, from top to bottom, respectively. It can be seen that the Volterra system output is severely distorted by impulsive noise. The PWM filter output PSD yields the desired PSD with slight distortions. As in the time domain, the PWMy filter output PSD gives the best spectral performance with the least distortions and clearly defined frequency components.

B. Image Processing Application

The proposed PWMy filter structure is also utilized in an image processing application. *Quadratic Volterra* (QV) filters utilized in unsharp masking scenario [12] yield better results than conventional linear techniques [12]. The QV filter output used for extracting edges and features is given by [12]: $\mathcal{F}[I_{i,j}] = 3I_{i,j}^2 - 0.5I_{i+1,j+1}I_{i-1,j-1} - 0.5I_{i+1,j-1}I_{i-1,j+1} - I_{i+1,j}I_{i-1,j} - I_{i,j+1}I_{i,j-1}$. The filter output is scaled by λ and added to the original image, $I_e(i,j) = I(i,j) + \lambda\mathcal{F}[I(i,j)]$, to obtain the edge enhanced image, I_e. The image "Lena" and QV filter (with $\lambda = 0.002$ [12]) edge enhanced image are given in Fig. 4(a) and (b), respectively. Using the *polynomial myriadization* technique, the *Quadratic Weighted Myriad* (QWMy) filter for this specific application is obtained: $\mathcal{F}[I_{i,j}] = \text{MYRIAD}\left(K; 3 \circ I_{i,j}^2, -0.5 \circ I_{i+1,j+1}I_{i-1,j-1}, -0.5 \circ I_{i+1,j-1}I_{i-1,j+1}, -1 \circ I_{i+1,j}I_{i-1,j}, -1 \circ I_{i,j+1}I_{i,j-1}\right)$. The identical enhanced image is obtained with QWMy filtering and $K = 100000$ and $\lambda = 0.012$, Fig. 4(c).

Both filters are also used to enhance the image corrupted by additive Gaussian noise ($\sigma^2 = 100$) [12] shown in Fig. 4(d). The enhanced images are given in Fig. 4(e) and (f) for the QV and QWMy ($K = 1$) filter cases, respectively. Inspection of the images shows that the QWMy output contains less overshoot and ringing, as well as more consistent uniform regions. These observations are consistent with the L_1 norm error measurements, which are 21.0305 and 16.9479 for the QV and QWMy filter cases, respectively. Thus, the QWMy filter provides a 19.41% performance gain over the QV filter.

V. Conclusions

The higher-order statistics of *bell-shaped* Cauchy statistics, including probability density functions of cross and square terms, and their tail heaviness order is analyzed. Motivated by these studies and the optimality of the weighted myriad filter under practical impulsive noise environments, a novel Polynomial Weighted Myriad (PWMy) filter is proposed for impulsive noise environments. Some properties of the proposed filter are presented. Adaptive and simple myriadization procedures are given. The proposed filter structure is tested through simulations and compared with the conventional Volterra and polynomial weighted median filtering [6]. The simulation results show the superiority of the proposed PWMy algorithm.

References

[1] M. Schetzen, *The Volterra and Wiener Theories of Nonlinear Systems*. New York: Wiley, 1980, .

[2] V. J. Mathews and G. L. Sicuranza, *Polynomial Signal Processing*. Chichester, U.K.: Wiley, 2000.

[3] I. Pitas and A. Venetsanopoulos, *Nonlinear Digital Filters: Principles and Application*. Norwell, MA: Kluwer, 1990.

[4] P. Koukoulas and N. Kalouptsidis, "Second order volterra system identification," *IEEE Trans. Signal Process.*, vol. 48, no. 12, pp. 3574–3577, Dec. 2000.

[5] Y. S. Cho and E. J. Powers, "Quadratic system identification using higher order spectra of i.i.d. signals," *IEEE Trans. Signal Process.*, vol. 42, no. 5, pp. 1268–1271, May 1994.

[6] K. E. Barner and T. C. Aysal, "Polynomial weighted median filtering," *IEEE Trans. Signal Process.*, vol. 54, no. 2, pp. 636–650, Feb. 2006.

[7] J. G. Gonzalez, D. L. Lau, and G. R. Arce, "Toward a general theory of robust nonlinear filtering: Selection filters," in *Proc. 1997 IEEE Int. Conf. Acoustics, Speech, Signal Process. (ICASSP)*, Munich, Germany, Apr. 21–24, 1997, pp. 3837–3840.

[8] J. G. Gonzalez and G. R. Arce, "Optimality of the myriad filter in practical impulsive-noise environments," *IEEE Trans. Signal Process.*, vol. 49, no. 2, pp. 438–441, Feb. 2001.

[9] C. Nikitas and M. Shao, *Signal Processing with Alpha-Stable Distributions and Applications*. New York: Wiley, 1995.

[10] S. Kalluri and G. R. Arce, "Adaptive weighted myriad filter algorithms for robust signal processing in α-stable environments," *IEEE Trans. Signal Process.*, vol. 46, no. 2, pp. 322–334, Feb. 1998.

[11] G. R. Arce, *Nonlinear Signal Processing: A Statistical Approach*. New York: Wiley, 2005.

[12] S. Thurnhofer and S. K. Mitra, "A general framework for quadratic volterra filters for edge enhancement," *IEEE Trans. Image Process.*, vol. 5, no. 6, pp. 950–963, Jun 1996.

Doubly Constrained Robust Capon Beamformer With Ellipsoidal Uncertainty Sets

Amir Beck and Yonina C. Eldar

***Abstract*—The doubly constrained robust (DCR) Capon beamformer with a *spherical* uncertainty set was introduced and studied by Stoica and Wang. Here, we consider the generalized DCR problem (GDCR) in which the uncertainty set is an *ellipsoid* rather than a sphere. Although, as noted previously by Stoica and Wang, this problem is nonconvex and appears to be intractable, we show that it can be solved efficiently. In fact, we prove that the GDCR beamformer can be obtained as a solution to a convex optimization problem. To this end, we first derive a strong duality result for nonconvex quadratic programs with two quadratic constraints over the complex domain. Specializing the results to our context leads to a semidefinite programming formulation of the GDCR beamformer.**

***Index Terms*—Nonconvex quadratic optimization, robust Capon beamforming, S-lemma, strong duality.**

I. Introduction

Beamforming methods for processing temporal sensor array measurements are used extensively in a variety of areas such as radar, sonar and wireless communications [3]. One of its goals is to estimate a source signal amplitude $s(t)$ from N array observations $\boldsymbol{y}(t)$, where

$$\boldsymbol{y}(t) = s(t)\boldsymbol{a} + \boldsymbol{e}(t), \quad 1 \le t \le N. \tag{1}$$

Manuscript received June 14, 2005; revised April 2, 2006. The associate editor coordinating the review of this manuscript and approving it for publication was Dr. A. Rahim Leyman. This work was supported in part by the Israel Science Foundation and by the EU 6th framework programme, via the NEWCOM network of excellence.

A. Beck is with the Department of Industrial Engineering and Management, The Technion—Israel Institute of Technology, Haifa 32000, Israel (e-mail: becka@ie.technion.ac.il).

Y. C. Eldar is with the Department Electrical Engineering, The Technion—Israel Institute of Technology, Haifa 32000, Israel (e-mail: yonina@ee.technion.ac.il).

Color version of Fig. 1 is available online at http://ieeexplore.ieee.org.

Digital Object Identifier 10.1109/TSP.2006.885729

Here $\boldsymbol{a} \in \mathbb{C}^n$ is the length-n signal steering vector, and $\boldsymbol{e}(t)$ is a noise vector that captures both the interference and the random noise. A common strategy to estimating $s(t)$ is to use a linear beamformer with weights $\boldsymbol{w}$ that are chosen to maximize the signal-to-interference+noise ratio (SINR).

If the steering vector $\boldsymbol{a}$ and the covariance matrix $\boldsymbol{R}$ of the noise are known exactly, then the weights maximizing the SINR are given by

$$\boldsymbol{w} = \frac{\boldsymbol{R}^{-1}\boldsymbol{a}}{\boldsymbol{a}^*\boldsymbol{R}^{-1}\boldsymbol{a}}. \tag{2}$$

In practice, the covariance $\boldsymbol{R}$ is typically unknown, and is instead replaced by an estimate, such as the sample covariance of the measurements. Recently, there has also been considerable interest in robust beamforming methods that are designed to compensate for imperfect knowledge of the array steering vector [1], [4]–[6]. The uncertainty in $\boldsymbol{a}$ can be taken into account by treating it as a random vector with known second-order statistics [7]–[9]. Alternatively, $\boldsymbol{a}$ can be modeled as a deterministic vector that lies in an ellipsoid centered at a nominal steering vector $\boldsymbol{a}_0$ [1], [2], [5], [6]. The goal then is to design a robust beamformer that yields good SINR for all possible values of $\boldsymbol{a}$ in the uncertainty set.

Here, we focus on the robust Capon beamforming problem introduced in [1], in which it is assumed that $\boldsymbol{a}$ lies in an ellipsoidal set. In this method, the beamforming weights are chosen according to (2) where the unknown steering vector $\boldsymbol{a}$ is replaced by the solution to

$$\min_{\boldsymbol{a}\in\mathbb{C}^n}\{\boldsymbol{a}^*\boldsymbol{R}^{-1}\boldsymbol{a} : (\boldsymbol{a}-\boldsymbol{a}_0)^*\boldsymbol{D}(\boldsymbol{a}-\boldsymbol{a}_0) \le 1\} \tag{3}$$

where $\boldsymbol{D}$ is a given positive semidefinite matrix. The robust Capon beamformer was later extended to include norm constraints on the steering vector, leading to the *doubly constrained robust (DCR) Capon beamformer* [2]:

$$(\text{DCR}) \quad \min_{\boldsymbol{a}\in\mathbb{C}^n}\{\boldsymbol{a}^*\boldsymbol{R}^{-1}\boldsymbol{a} : \|\boldsymbol{a}\|^2 = n, \|\boldsymbol{a}-\boldsymbol{a}_0\|^2 \le \epsilon\}. \tag{4}$$

The solution of both (3) and (4) reduces to a simple root-finding problem of a *single variable* monotone function.

In the derivation of the DCR beamformer, it was explicitly assumed that the uncertainty set is spherical, and not ellipsoidal as in (3). However, ellipsoids can often provide a more accurate description of the uncertainty than spheres. One example is when the uncertainty set is constructed from repeated measurements of the array manifold using the mean and covariance of the measurements; see [6] for detailed methods that can be used to derive an appropriate uncertainty ellipsoid. A natural extension to the DCR beamformer is to include ellipsoidal sets, which leads to a generalized version of DCR:

$$(\text{GDCR}) \quad \begin{aligned} \min_{\boldsymbol{a}\in\mathbb{C}^n} \quad & \boldsymbol{a}^*\boldsymbol{R}^{-1}\boldsymbol{a} \\ \text{s.t.} \quad & \|\boldsymbol{a}\|^2 = n, \\ & (\boldsymbol{a}-\boldsymbol{a}_0)^*\boldsymbol{D}(\boldsymbol{a}-\boldsymbol{a}_0) \le \epsilon. \end{aligned} \tag{5}$$

A key difficulty with (5) is its nonconvexity due to the nonlinear *equality* constraint $\|\boldsymbol{a}\|^2 = n$. Another obstacle arises from the fact that using a Lagrange multiplier approach, the solution of (5) seems to involve a two-dimensional search, as noted in [2]:

> "However, it appears that DCR is not as easy to generalize to the case of ellipsoidal uncertainty sets as such a generalization would require a two-dimensional search to determine the Lagrange multipliers…."

Here, we treat the GDCR problem (5) and show that although it is nonconvex, strong duality holds. As a result, the value of (5) is equal to the value of a corresponding semidefinite program (SDP) [10], which can be solved efficiently using interior point methods. Furthermore, we show how to extract the solution of the primal problem from the solution of the dual problem. The special structure of the SDP allows it to be solved in a computational effort of $O(n^{3.5})$. Using these results we can determine the GDCR beamformer efficiently without having to employ ad hoc searches.

To develop the GDCR beamformer, we consider a more general optimization problem in which we seek to minimize a quadratic function subject to a quadratic inequality constraint, and a quadratic equality constraint. We do not assume convexity of any of the quadratic functions. By adapting a recently developed methodology [11] for quadratic problems with two *inequality* constraints to our context, we show that under mild conditions, strong duality holds for this nonconvex class of problems and relate the primal and dual solutions.

We emphasize that our purpose in this correspondence is to generalize the DCR beamformer to ellipsoid uncertainty sets, which are used in other formulations of robust beamforming. Our intention is not to endorse this particular beamforming method or to claim that it is superior to other approaches. We do, however, believe that if the DCR beamformer is chosen in a particular application, then it may be beneficial to include ellipsoidal uncertainty sets as well. To illustrate this point, in Section IV, we present an example taken from [6] where the uncertainty is constructed from measurements of the array manifold. In this case, there may be an advantage to using ellipsoidal sets over spherical ones that capture the covariance of the measurements.

The outline of the correspondence is as follows. Section II begins with the description of the general nonconvex quadratic problem with two quadratic constraints (Q2P). Using an extended version of the so-called S-lemma, we show, in Section III, that under some mild conditions, strong duality holds for (Q2P). We then present a method for calculating the optimal solution of (Q2P) from the dual solution. Finally, in Section IV, we show that in the GDCR problem the conditions for strong duality are met, so that an efficient solution can be obtained in polynomial time.

Throughout the correspondence, we use the following notation: Vectors are denoted by boldface lowercase letters, and matrices by boldface uppercase letters. For two matrices $\boldsymbol{A}$ and $\boldsymbol{B}$, $\boldsymbol{A} \succ (\succeq) \boldsymbol{B}$ means that $\boldsymbol{A}-\boldsymbol{B}$ is positive (semi)definite. Instead of using an inf/sup notation, we use a min/max notation.[1] The real and imaginary part of scalars, vectors, or matrices are denoted by $\Re(\cdot)$ and $\Im(\cdot)$, respectively. For an optimization problem $(P) : \min / \max\{f(\boldsymbol{x}) : \boldsymbol{x} \in C\}$, we denote the value of the optimal objective function by $\mathrm{val}(P)$. When (P) is infeasible, we define $\mathrm{val}(P) = \infty$. We follow the MATLAB convention and use ";" for adjoining scalars, vectors, or matrices in a column.

II. Problem Formulation and Mathematical Background

The GDCR beamforming problem of (5) can be viewed as a special case of a nonconvex quadratic minimization with two quadratic constraints in the complex domain, as follows:

$$(\text{Q2P}) \quad \min_{\boldsymbol{z}\in\mathbb{C}^n}\{f_3(\boldsymbol{z}) : f_1(\boldsymbol{z}) \ge 0, f_2(\boldsymbol{z}) = 0\}. \tag{6}$$

Here, $f_j : \mathbb{C}^n \to \mathbb{R}$ is given by

$$f_j(\boldsymbol{z}) = \boldsymbol{z}^*\boldsymbol{A}_j\boldsymbol{z} + 2\Re(\boldsymbol{b}_j^*\boldsymbol{z}) + c_j \tag{7}$$

where $\boldsymbol{A}_j$ are Hermitian matrices, i.e., $\boldsymbol{A}_j = \boldsymbol{A}_j^*$, $\boldsymbol{b}_j \in \mathbb{C}^n$, and $c_j \in \mathbb{R}$. Note that neither the constraints nor the objective function are assumed to be convex, so that we make no assumptions on the Hermitian matrices $\boldsymbol{A}_j$.

Since problem (6) is not convex, it is not clear at first sight how to obtain efficient methods for its solution. One of the attributes of convexity is that it implies that the values of the primal and dual problems

[1]The fact that we use this notation does not mean that we assume that the optimum is attained and/or finite.

are equal (strong duality) [12]. Strong duality is, in many cases, the key ingredient in deriving efficient solution methods. Fortunately, we will show that even though (6) is not convex, strong duality holds for this class of problems under very mild conditions. In our derivation, we use a recently developed methodology [11] for quadratic problems with two *inequality* constraints and generalize this approach to our setting.

It is interesting to note that for quadratic problems with two quadratic constraints in the *real domain*, strong duality does not hold except for some special cases [11], [13]. On the other hand, for problems with a *single* quadratic constraint, strong duality holds under mild conditions both in the real and complex domains [14], [15].

The key ingredient in proving strong duality of (Q2P) is the extended S-lemma.

Theorem II.1 (Extended S-Lemma [16]): Let

$$f_j(z) = z^*\boldsymbol{A}_j z + 2\Re(\boldsymbol{b}_j^* z) + c_j, \quad z \in \mathbb{C}^n, j = 1,2,3$$

where $\boldsymbol{A}_j$ are $n \times n$ Hermitian matrices, $\boldsymbol{b}_j \in \mathbb{C}^n$, and $c_j \in \mathbb{R}$. Suppose that there exists $\tilde{z} \in \mathbb{C}^n$ such that $f_1(\tilde{z}) > 0$, $f_2(\tilde{z}) > 0$ and a $\tilde{\boldsymbol{w}} \in \mathbb{C}^n$ such that $f_1(\tilde{\boldsymbol{w}}) > 0$ and $f_2(\tilde{\boldsymbol{w}}) < 0$. Then, the following two claims are equivalent:

1) $f_3(z) \geq 0$ for every $z \in \mathbb{C}^n$ such that $f_1(z) \geq 0$ and $f_2(z) = 0$;
2) there exists $\alpha \geq 0$ and $\beta \in \mathbb{R}$ such that

$$\begin{pmatrix} \boldsymbol{A}_3 & \boldsymbol{b}_3 \\ \boldsymbol{b}_3^* & c_3 \end{pmatrix} \succeq \alpha \begin{pmatrix} \boldsymbol{A}_1 & \boldsymbol{b}_1 \\ \boldsymbol{b}_1^* & c_1 \end{pmatrix} + \beta \begin{pmatrix} \boldsymbol{A}_2 & \boldsymbol{b}_2 \\ \boldsymbol{b}_2^* & c_2 \end{pmatrix}.$$

It is important to realize that Theorem II.1 is not true in the real domain. For example, the following implication in $\mathbb{R}$ is obvious:

$$2x \geq 2 \text{ for every } x \in \mathbb{R} \text{ such that } 2x \geq 0, x^2 = 1.$$

The regularity conditions of Theorem II.1 are satisfied. However, a simple argument shows that there are no $\alpha \geq 0$ and $\beta \in \mathbb{R}$ such that

$$\begin{pmatrix} 0 & 1 \\ 1 & -2 \end{pmatrix} \succeq \alpha \begin{pmatrix} 0 & 1 \\ 1 & 0 \end{pmatrix} + \beta \begin{pmatrix} 1 & 0 \\ 0 & -1 \end{pmatrix}. \tag{8}$$

Consequently, the results we develop are valid only for problems defined on the complex domain, as is the case in GDCR beamforming.

III. Strong Duality and Optimality Conditions

Using standard manipulations, it can be readily shown that the Lagrangian dual of (Q2P) is given by

$$(D) \max_{\alpha \geq 0, \beta, \lambda} \left\{ \lambda \middle| \begin{pmatrix} \boldsymbol{A}_3 & \boldsymbol{b}_3 \\ \boldsymbol{b}_3^* & c_3 - \lambda \end{pmatrix} \succeq \alpha \begin{pmatrix} \boldsymbol{A}_1 & \boldsymbol{b}_1 \\ \boldsymbol{b}_1^* & c_1 \end{pmatrix} + \beta \begin{pmatrix} \boldsymbol{A}_2 & \boldsymbol{b}_2 \\ \boldsymbol{b}_2^* & c_2 \end{pmatrix} \right\}. \tag{9}$$

Theorem III.1 below states that if (Q2P) is strictly feasible then val(Q2P) $=$ val(D) even when the value is equal to $-\infty$. Problem (Q2P) is said to be *strictly feasible* if there exists $\tilde{z}, \tilde{\boldsymbol{w}} \in \mathbb{C}^n$ such that $f_1(\tilde{z}) > 0$, $f_2(\tilde{z}) > 0$ and $f_1(\tilde{\boldsymbol{w}}) > 0$, $f_2(\tilde{\boldsymbol{w}}) < 0$.

Theorem III.1 (Strong Duality): Suppose that (Q2P) is strictly feasible. Then, we have the following:

1) if val(Q2P) is finite, then the maximum of problem (D) is attained and val(Q2P) $=$ val(D);
2) val(Q2P) $> -\infty$ if and only if problem (D) is feasible.

Proof:

1. Suppose first that val(Q2P) is finite. Then

$$\text{val(Q2P)} = \max_{\lambda}\{\lambda : \text{val(Q2P)} \geq \lambda\}. \tag{10}$$

Now, the statement val(Q2P) $\geq \lambda$ holds true if and only if the implication

$$f_1(z) \geq 0, f_2(z) = 0 \Rightarrow f_3(z) \geq \lambda$$

is valid. By Theorem II.1, this is equivalent to the claim that there exists $\alpha \geq 0$ and β such that

$$\begin{pmatrix} \boldsymbol{A}_3 & \boldsymbol{b}_3 \\ \boldsymbol{b}_3^* & c_3 - \lambda \end{pmatrix} \succeq \alpha \begin{pmatrix} \boldsymbol{A}_1 & \boldsymbol{b}_1 \\ \boldsymbol{b}_1^* & c_1 \end{pmatrix} + \beta \begin{pmatrix} \boldsymbol{A}_2 & \boldsymbol{b}_2 \\ \boldsymbol{b}_2^* & c_2 \end{pmatrix}. \tag{11}$$

Therefore, by replacing the constraint in the maximization problem (10) with the LMI (11), we obtain that val(Q2P) $=$ val(D). The maximum of (D) is attained at $(\bar{\lambda}, \bar{\alpha}, \bar{\beta})$, where $\bar{\lambda}$ is the (finite) value val(Q2P) and $\bar{\alpha} \geq 0, \bar{\beta}$ are the corresponding constants that satisfy the LMI (11) for $\lambda = \bar{\lambda} =$ val(Q2P).

2. Note that val(Q2P) $> -\infty$ if and only if there exists $\lambda \in \mathbb{R}$ such that val(Q2P) $\geq \lambda$, which is equivalent to

$$f_1(z) \geq 0, f_2(z) = 0 \Rightarrow f_3(z) \geq \lambda.$$

By Theorem II.1, the latter implication is the same as (11), which is equivalent to feasibility of (D). ■

We now derive necessary and sufficient optimality conditions on the solution to (Q2P).

Theorem III.2 (Optimality Conditions): Suppose that (Q2P) is strictly feasible and that its minimum is attained. Let $(\bar{\alpha}, \bar{\beta}, \bar{\lambda})$ be an optimal solution of (D). Then $\bar{z}$ is an optimal solution of (Q2P) if and only if

$$(\boldsymbol{A}_3 - \bar{\alpha}\boldsymbol{A}_1 - \bar{\beta}\boldsymbol{A}_2)\bar{z} = \bar{\alpha}\boldsymbol{b}_1 + \bar{\beta}\boldsymbol{b}_2 - \boldsymbol{b}_3 \tag{12}$$

$$f_1(\bar{z}) \geq 0, f_2(\bar{z}) = 0 \tag{13}$$

$$\bar{\alpha} f_1(\bar{z}) = 0. \tag{14}$$

Proof: From the strong duality result (Theorem III.1) and from saddle point optimality conditions (see, e.g., [17, Theorem 6.2.5]), it follows that $\bar{z}$ is an optimal solution of (Q2P) if and only if

$$\begin{aligned} &\bar{z} \in \operatorname{argmin} \mathcal{L}(z, \bar{\alpha}, \bar{\beta}) \\ &f_1(\bar{z}) \geq 0, f_2(\bar{z}) = 0 \\ &\bar{\alpha} f_1(\bar{z}) = 0 \end{aligned} \tag{15}$$

where $\mathcal{L}(z, \alpha, \beta) = f_3(z) - \alpha f_1(z) - \beta f_2(z)$. Note that (15) implies in particular that $\min_z \mathcal{L}(z, \bar{\alpha}, \bar{\beta}) > -\infty$. We now rely on the following lemma.

Lemma III.1: Let $f : \mathbb{C}^n \to \mathbb{R}$ be the quadratic function $f(z) = z^*\boldsymbol{A}z + 2\Re(b^*z) + c$, where $\boldsymbol{A} = \boldsymbol{A}^* \in \mathbb{C}^{n \times n}$, $\boldsymbol{b} \in \mathbb{C}^n$ and $c \in \mathbb{R}$. Suppose that $\min_{z \in \mathbb{C}^n} f(z) > -\infty$. Then, $\boldsymbol{A}$ is positive semidefinite and the set of optimal solutions is given by $\{z : \boldsymbol{A}z + \boldsymbol{b} = 0\}$.

By Lemma III.1, condition (15) is equivalent to (12), completing the proof. ■

A. Finding an Explicit Solution of (Q2P)

We now use the optimality conditions of Theorem III.2 in order to describe a method for extracting the solution of (Q2P) from the solution of the dual problem (D).

Suppose that (Q2P) is strictly feasible and that the minimum is finite. From Theorem III.2, $\bar{z}$ is an optimal solution if it satisfies (12)–(14). If $\boldsymbol{A}_3 - \bar{\alpha}\boldsymbol{A}_1 - \bar{\beta}\boldsymbol{A}_2 \succ \boldsymbol{0}$, then the (unique) solution to the primal problem (Q2P) is

$$\bar{z} = -(\boldsymbol{A}_3 - \bar{\alpha}\boldsymbol{A}_1 - \bar{\beta}\boldsymbol{A}_2)^{-1}(\boldsymbol{b}_3 - \bar{\alpha}\boldsymbol{b}_1 - \bar{\beta}\boldsymbol{b}_2).$$

Next, suppose that $\boldsymbol{A}_3 - \bar{\alpha}\boldsymbol{A}_1 - \bar{\beta}\boldsymbol{A}_2$ is positive semidefinite but not positive definite. In this case, (12) can be written as $\bar{z} = \boldsymbol{B}\boldsymbol{w} + \boldsymbol{a}$, where the columns of $\boldsymbol{B}$ form a basis for the null space of $\boldsymbol{A}_3 - \bar{\alpha}\boldsymbol{A}_1 - \bar{\beta}\boldsymbol{A}_2$ and $\boldsymbol{a} = -(\boldsymbol{A}_3 - \bar{\alpha}\boldsymbol{A}_1 - \bar{\beta}\boldsymbol{A}_2)^{\dagger}(\boldsymbol{b}_3 - \bar{\alpha}\boldsymbol{b}_1 - \bar{\beta}\boldsymbol{b}_2)$ is a solution of (12).

TABLE I
CASES OF THE QUADRATIC FEASIBILITY PROBLEM

No.	Case	Feasibility Problem
I	$\bar{\alpha}=0$	$g_1(\boldsymbol{w})\geq 0$ and $g_2(\boldsymbol{w})=0$
II	$\bar{\alpha}>0$	$g_1(\boldsymbol{w})=0$ and $g_2(\boldsymbol{w})=0$

It follows that $\bar{z}=\boldsymbol{B}\bar{\boldsymbol{w}}+\boldsymbol{a}$ is an optimal solution to (Q2P) if and only if conditions (13) and (14) of Theorem III.2 are satisfied, i.e.,

$$g_1(\bar{\boldsymbol{w}})\geq 0,\ g_2(\bar{\boldsymbol{w}})=0,\ \bar{\alpha}g_1(\bar{\boldsymbol{w}})=0 \tag{16}$$

where $g_j(\boldsymbol{w})\equiv f_j(\boldsymbol{B}\boldsymbol{w}+\boldsymbol{a})$. We are left with the problem of finding a vector that is a solution of a system of two quadratic equalities or inequalities as described in Table I. This problem will be called the *quadratic feasibility problem*.

We summarize the above discussion in the following theorem.

Theorem III.3: Suppose that problem (Q2P) is strictly feasible and that its minimum is attained. Let $(\bar{\alpha},\bar{\beta},\bar{\lambda})$ be an optimal solution of problem (D). Then, we have the following:

1) if $\boldsymbol{A}_3-\bar{\alpha}\boldsymbol{A}_1-\bar{\beta}\boldsymbol{A}_2\succ \mathbf{0}$, then the (unique) optimal solution of (Q2P) is given by

$$\bar{z}=-(\boldsymbol{A}_3-\bar{\alpha}\boldsymbol{A}_1-\bar{\beta}\boldsymbol{A}_2)^{-1}(\boldsymbol{b}_3-\bar{\alpha}\boldsymbol{b}_1-\bar{\beta}\boldsymbol{b}_2);$$

2) if $\boldsymbol{A}_3-\bar{\alpha}\boldsymbol{A}_1-\bar{\beta}\boldsymbol{A}_2\succeq \mathbf{0}$ but not positive definite, then the solutions of (Q2P) are given by $z=\boldsymbol{B}\boldsymbol{w}+\boldsymbol{a}$, where $\boldsymbol{B}\in\mathbb{C}^{n\times d}$ is a matrix whose columns form a basis for the null space of $\boldsymbol{A}_3-\bar{\alpha}\boldsymbol{A}_1-\bar{\beta}\boldsymbol{A}_2$, $\boldsymbol{a}$ is a solution of system (12), and $\boldsymbol{w}\in\mathbb{C}^d$ is any solution of the quadratic feasibility problem (16), where d is the dimension of the null space.

The computational effort required for the solution of (Q2P) is dominated by the amount of operations involved in solving the SDP (D). The fact that (D) has only three variables implies that solving it requires $O(n^{3.5})$ computer operations (see [18, p. 423] for details).

B. Solving the Quadratic Feasibility Problem

We now develop a method for solving the two instances of the quadratic feasibility problem described in Table I, under the condition that f_2 is a strongly concave quadratic function,[2] i.e., $\boldsymbol{A}_2\prec\mathbf{0}$. Note that this condition is naturally satisfied for the GDCR problem (5). The strong concavity of $g_2(\boldsymbol{w})=f_2(\boldsymbol{B}\boldsymbol{w}+\boldsymbol{a})$ follows immediately. All of these feasibility problems have at least one solution, a fact that follows from their construction. By applying an appropriate linear transformation on g_2, we can assume without loss of generality that $g_2(\boldsymbol{w})=\gamma-\|\boldsymbol{w}\|^2$ $(\gamma\geq 0)$.

Our approach for solving the quadratic feasibility problem will be to use the solution of optimization problems of the following type:

$$\min_{\boldsymbol{z}\in\mathbb{C}^n}\{\boldsymbol{z}^*\mathbf{Q}\boldsymbol{z}+2\Re(\boldsymbol{f}^*\boldsymbol{z}):\|z\|^2=\gamma\} \tag{17}$$

where $\mathbf{Q}=\mathbf{Q}^*\in\mathbb{C}^n$ and $\boldsymbol{f}\in\mathbb{C}^n$. Problem (17) is closely related to the trust region subproblem (the only difference is that there is an equality constraint and not an inequality constraint).[3] A complete description of the solution to (17) can be found in, e.g., [19, p. 825].

We split our analysis according to the two different cases.

[2]Thus, the corresponding constraint is strongly convex.

[3]More details on the trust region subproblem can be found, e.g., in [14], and [15].

1) Case I: Here, we need to solve the quadratic feasibility problem

$$g_1(\boldsymbol{w})\geq 0,\quad \|\boldsymbol{w}\|^2=\gamma. \tag{18}$$

Since (18) has at least one solution, it follows that the value of the optimization problem

$$\max\{g_1(\boldsymbol{w}):\|\boldsymbol{w}\|^2=\gamma\} \tag{19}$$

is nonnegative and therefore any solution of (19) is a solution to (18).

2) Case II: The feasibility problem now is

$$g_1(\boldsymbol{w})=0,\quad \|\boldsymbol{w}\|^2=\gamma. \tag{20}$$

To find a solution to (20), we first consider the following optimization problems:

$$\min\{g_1(\boldsymbol{w}):\|\boldsymbol{w}\|^2=\gamma\},\quad \max\{g_1(\boldsymbol{w}):\|\boldsymbol{w}\|^2=\gamma\}. \tag{21}$$

Let $\boldsymbol{w}^0$ and $\boldsymbol{w}^1$ be solutions to the minimization and maximization problems of (21) respectively. Then $\|\boldsymbol{w}^0\|^2=\|\boldsymbol{w}^1\|^2=\gamma$. Since (20) must have at least one solution, we conclude that $g_1(\boldsymbol{w}^0)\leq 0\leq g_1(\boldsymbol{w}^1)$. The analysis now depends on the relation between $\boldsymbol{w}^0$ and $\boldsymbol{w}^1$:

[1.] **$\boldsymbol{w}^0$ and $\boldsymbol{w}^1$ are linearly dependent.** Since $\boldsymbol{w}^0$ and $\boldsymbol{w}^1$ have the same norm, we conclude that $\boldsymbol{w}^1=e^{i\theta_0}\boldsymbol{w}^0$. Let $\mathcal{G}(\theta)\equiv g_1(e^{i\theta}\boldsymbol{w}^0)$ $(\theta\in[0,\theta_0])$. Then, $\mathcal{G}$ is a continuous function over the interval $[0,\theta_0]$ that satisfies $\mathcal{G}(0)=g_1(\boldsymbol{w}^0)\leq 0$, $\mathcal{G}(\theta_0)=g_1(e^{i\theta_0}\boldsymbol{w}^0)=g_1(\boldsymbol{w}^1)\geq 0$. Therefore, there exists $\bar{\theta}\in[0,\theta_0]$ such that $\mathcal{G}(\bar{\theta})=0$. The vector $\bar{\boldsymbol{w}}=e^{i\bar{\theta}}\boldsymbol{w}^0$ is a solution to (20).

[2.] **$\boldsymbol{w}^0$ and $\boldsymbol{w}_1$ are linearly independent**. Here, we can define

$$\boldsymbol{u}(\eta)=\boldsymbol{w}^0+\eta(\boldsymbol{w}^1-\boldsymbol{w}^0),\quad \boldsymbol{w}(\eta)=\sqrt{\gamma}\frac{\boldsymbol{u}(\eta)}{\|\boldsymbol{u}(\eta)\|},\ \ \eta\in[0,1].$$

By the definition of $\boldsymbol{w}(\eta)$, we have that $\|\boldsymbol{w}(\eta)\|^2=\gamma$ for every $\eta\in[0,1]$ and $g_1(\boldsymbol{w}(0))\leq 0\leq g_1(\boldsymbol{w}(1))$. All that is left is to find a root to the scalar equation $g_1(\boldsymbol{w}(\eta))=0, \eta\in[0,1]$, which can be written as

$$\gamma\frac{\boldsymbol{u}(\eta)^*\boldsymbol{A}_2\boldsymbol{u}(\eta)}{\|\boldsymbol{u}(\eta)\|^2}+\frac{2\sqrt{\gamma}}{\|\boldsymbol{u}(\eta)\|}\Re(\boldsymbol{b}_2^*\boldsymbol{u}(\eta))+c_2=0,\quad \eta\in[0,1]. \tag{22}$$

It is elementary to see that all the solutions of (22) also satisfy the following *quartic* scalar equation:

$$\left(\gamma\boldsymbol{u}(\eta)^*\boldsymbol{A}_2\boldsymbol{u}(\eta)+c_2\|\boldsymbol{u}(\eta)\|^2\right)^2=4\gamma\|\boldsymbol{u}(\eta)\|^2(\Re(\boldsymbol{b}_2^*\boldsymbol{u}(\eta)))^2. \tag{23}$$

The solution of the quadratic feasibility problem is given by $w(\eta)$, where η is one of the solutions to (23). Notice that (23) has at most four solutions, which have explicit algebraic expressions.

IV. GENERALIZED DCR BEAMFORMER

The GDCR beamformer of (5) is a special case of (Q2P), and therefore can be solved by using the techniques of the previous section.

The first step to obtaining a solution is formulating the dual problem. This can be easily obtained by substituting $\boldsymbol{A}_1-\boldsymbol{D}$, $\boldsymbol{A}_2=\boldsymbol{I}$, $\boldsymbol{A}_3=\boldsymbol{R}^{-1}$, $\boldsymbol{b}_1=\boldsymbol{D}\boldsymbol{a}_0$, $\boldsymbol{b}_2=\boldsymbol{b}_3=\mathbf{0}$, $c_1=\epsilon-\boldsymbol{a}_0^*\boldsymbol{D}\boldsymbol{a}_0$, $c_2=-n$, $c_3=0$ in problem (D), resulting in

$$\max_{\alpha\geq 0,\beta,\lambda}\left\{\lambda\left|\begin{pmatrix}\boldsymbol{R}^{-1} & \mathbf{0}\\ \mathbf{0} & -\lambda\end{pmatrix}\succeq\alpha\begin{pmatrix}-\boldsymbol{D}+\beta\boldsymbol{I} & \boldsymbol{D}\boldsymbol{a}_0\\ \boldsymbol{a}_0^*\boldsymbol{D} & \epsilon-\boldsymbol{a}_0^*\boldsymbol{D}\boldsymbol{a}_0-\beta n\end{pmatrix}\right.\right\}. \tag{24}$$

The GDCR beamformer can then be derived by the following steps.

1. Find an optimal solution $(\bar{\alpha},\bar{\beta},\bar{\lambda})$ of the SDP **(24)**.

2. If

$$\boldsymbol{R}^{-1} + \bar{\alpha}\boldsymbol{D} - \bar{\beta}\boldsymbol{I} \succ \boldsymbol{0} \tag{25}$$

then the solution of the GDCR problem (5) is

$$\bar{\boldsymbol{a}} = \bar{\alpha}(\boldsymbol{R}^{-1} + \bar{\alpha}\boldsymbol{D} - \bar{\beta}\boldsymbol{I})^{-1}\boldsymbol{D}\boldsymbol{a}_0.$$

3. Otherwise, $\bar{\boldsymbol{a}}$ is any solution of the feasibility problem

$$(\boldsymbol{R}^{-1} + \bar{\alpha}\boldsymbol{D} - \bar{\beta}\boldsymbol{I})\bar{\boldsymbol{a}} = \bar{\alpha}\boldsymbol{D}\boldsymbol{a}_0, \tag{26}$$

$$(\bar{\boldsymbol{a}} - \boldsymbol{a}_0)^*\boldsymbol{D}(\bar{\boldsymbol{a}} - \boldsymbol{a}_0)^* \le \epsilon, \quad \|\bar{\boldsymbol{a}}\|^2 = n \tag{27}$$

which can be obtained by using the techniques of Section III-B.

The validity of the above procedure relies on the assumption that the regularity conditions of Theorem III.3 hold true. We now prove that in fact these conditions are automatically met for the GDCR problem.

Proposition IV.1: The GDCR problem (5) is strictly feasible and attains its minimum.

Proof: The minimum of the GDCR problem is attained since its feasible set is compact due to the equality constraint. To prove strict feasibility, we need to show that there exist $\boldsymbol{b}, \boldsymbol{c} \in \mathbb{C}^n$ such that

$$\|\boldsymbol{b}\|^2 < n, \quad (\boldsymbol{b} - \boldsymbol{a}_0)^*\boldsymbol{D}(\boldsymbol{b} - \boldsymbol{a}_0) < \epsilon \tag{28}$$

$$\|\boldsymbol{c}\|^2 > n, \quad (\boldsymbol{c} - \boldsymbol{a}_0)^*\boldsymbol{D}(\boldsymbol{c} - \boldsymbol{a}_0) < \epsilon. \tag{29}$$

Using the fact that $\|\boldsymbol{a}_0\|^2 = n$, it follows by a simple substitution that $\boldsymbol{b} = \gamma_1\boldsymbol{a}_0$ and $\boldsymbol{c} = \gamma_2\boldsymbol{a}_0$ with γ_1 and γ_2 defined by

$$\gamma_1 = \begin{cases} \frac{1}{2}, & \boldsymbol{a}_0^*\boldsymbol{D}\boldsymbol{a}_0 = 0 \\ 1 - \frac{1}{2}\sqrt{\frac{\epsilon}{\boldsymbol{a}_0^*\boldsymbol{D}\boldsymbol{a}_0}}, & \boldsymbol{a}_0^*\boldsymbol{D}\boldsymbol{a}_0 \neq 0 \end{cases}$$

$$\gamma_2 = \begin{cases} 2, & \boldsymbol{a}_0^*\boldsymbol{D}\boldsymbol{a}_0 = 0 \\ 1 + \frac{1}{2}\sqrt{\frac{\epsilon}{\boldsymbol{a}_0^*\boldsymbol{D}\boldsymbol{a}_0}}, & \boldsymbol{a}_0^*\boldsymbol{D}\boldsymbol{a}_0 \neq 0 \end{cases}$$

satisfy (28) and (29). ■

A. Numerical Examples

We now present three numerical examples of the GDCR beamformer. The first two are "toy" examples which illustrate how to extract the solution to the GDCR problem from the dual solution when condition (25) is satisfied and when it is not. The third example, in which (25) is satisfied, represents a more typical array processing scenario and is taken from [6]; here, the uncertainty set is constructed from measurements of the array manifold. We compare the GDCR and DCR methods and show that there may be an advantage to using ellipsoidal sets that capture the covariance of the measurements. All the SDPs in this section were solved using SeDuMi [20].

1) Example 1: Consider the GDCR problem with $n = 2$ and the following data:

$$\boldsymbol{R}^{-1} = \begin{pmatrix} 3 & 1+i \\ 1-i & 4 \end{pmatrix}, \boldsymbol{D} = \begin{pmatrix} 2 & 1+i \\ 1-i & 4 \end{pmatrix},$$

$$\boldsymbol{a}_0 = \begin{pmatrix} 1 \\ -1 \end{pmatrix}, \epsilon = 2.$$

The solution of the dual problem of (5) is

$$\bar{\lambda} = 4.0343, \quad \bar{\alpha} = 0.152, \quad \bar{\beta} = 2.0082.$$

Note that $\bar{\lambda} = 4.0343$ is the optimal value and the fact that $\bar{\alpha}$ is positive implies that the first constraint is active (the second constraint is inherently active). In this example, we have $\boldsymbol{R}^{-1} + \bar{\alpha}\boldsymbol{D} - \bar{\beta}\boldsymbol{I} \succ \boldsymbol{0}$, and thus the optimal solution is

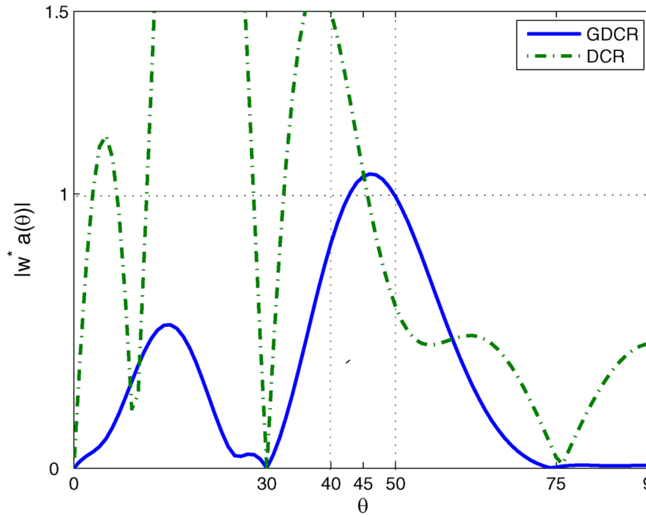

Fig. 1. Comparison of the GDCR and DCR beamformers.

$$\bar{\boldsymbol{a}} = \bar{\alpha}(\boldsymbol{R}^{-1} + \bar{\alpha}\boldsymbol{D} - \bar{\beta}\boldsymbol{I})^{-1}\boldsymbol{D}\boldsymbol{a}_0 = \begin{pmatrix} 1.0430 + 0.4271i \\ -0.8268 + 0.2144i \end{pmatrix}.$$

2) Example 2: Consider the GDCR problem (5) with

$$\boldsymbol{R} = \begin{pmatrix} 2 & -0.5 \\ -0.5 & 0.25 \end{pmatrix}, \boldsymbol{D} = \begin{pmatrix} 1 & 1 \\ 1 & 1 \end{pmatrix}, \boldsymbol{a}_0 = \begin{pmatrix} 1 \\ 1 \end{pmatrix}, n = 2, \epsilon = 1.$$

In this case, the dual solution is

$$\bar{\lambda} = 0.9377, \quad \bar{\alpha} = 0, \quad \bar{\beta} = -0.4689.$$

The eigenvalues of the matrix $\boldsymbol{R}^{-1} + \bar{\alpha}\boldsymbol{D} - \bar{\beta}\boldsymbol{I}$ are 0 and 8.0623. Thus, $\boldsymbol{R}^{-1} + \bar{\alpha}\boldsymbol{D} - \bar{\beta}\boldsymbol{I}$ is singular and in order to find an optimal solution we will transform the problem into a quadratic feasibility problem. The null space of $\boldsymbol{R}^{-1} + \bar{\alpha}\boldsymbol{D} - \bar{\beta}\boldsymbol{I}$ is spanned by the vector $\boldsymbol{u} = (-0.9665; 0.2567)$. Since in this example $\bar{\alpha} = 0$, it follows that the set of solutions to (26) is given by $\{\boldsymbol{a} = w\boldsymbol{u} : w \in \mathbb{C}\}$. From (27), w must satisfy

$$-|w|^2 + 2 = 0 \text{ and } -0.5038|w|^2 - 2.8392\Re(w) - 2 \ge 0.$$

A solution to the latter feasibility problem is the optimal solution of

$$\max_{w \in \mathbb{C}}\{-0.5038|w|^2 - 2.8392\Re(w) - 2 : |w|^2 = 2\}$$

which is given by $w = -\sqrt{2}$. Thus, the GDCR solution is $\boldsymbol{a} = w\boldsymbol{u} = (1.3688; -0.363)$.

3) Example 3: We now present a more realistic array processing problem taken from [6]. In this example, we consider a ten-element uniform linear array in which the spacing between the elements is half a wavelength. The noise vector $e(t)$ in (1) is comprised of two uncorrelated interfering signals with angles of arrival (AOA) equal to 30° and 75°. The signal-to-noise ratios (SNRs) of the signals are 40 and 20 dB, respectively. The noise is spatially and temporally white with an SNR of 20 dB. The actual array response is unknown; instead, we are given $N = 64$ random measurements of the array manifold where the AOAs of the desired user are drawn at random between 40° and 50°. The true steering vector is then estimated by using the GDCR method where $\boldsymbol{a}_0$ is chosen as the sample mean and $\boldsymbol{D}$ is the inverse sample covariance matrix. The covariance matrix is given by [6, eq. (48)] (with $\sigma_n^2 = 0.01$). The value of ϵ is chosen so that all the data points $\boldsymbol{a}(\theta_i)$ will be inside the ellipsoid. For comparison, we also implement the DCR beamformer where in this case $\boldsymbol{a}_0$ is as before, and ϵ is chosen so that all $\boldsymbol{a}(\theta_i)$ are inside $\{\boldsymbol{a} : \|\boldsymbol{a} - \boldsymbol{a}_0\|^2 \leq \epsilon\}$.

In Fig. 1, we plot the array response using the GDCR and DCR beamformers. As can be seen from the figure, the GDCR method has close to unity gain for all AOAs covered by the uncertainty ellipsoid. On the other hand, the gain of the DCR approach deteriorates for AOAs larger than 45°.

The point of this example is to illustrate the potential advantage in including ellipsoidal sets into the robust Capon formulation. Since the contribution of this correspondence is in the mathematical derivation of the GDCR method, a detailed application is beyond the scope. However, Fig. 1 demonstrates that at least in some cases it may be advantageous to include ellipsoidal sets.

REFERENCES

[1] J. Li, P. Stoica, and Z. Wang, "On robust capon beamforming and diagonal loading," *IEEE Trans. Signal Process.*, vol. 51, no. 7, pp. 1702–1715, Jul. 2003.

[2] ——, "Doubly constrained robust capon beamformer," *IEEE Trans. Signal Process.*, vol. 52, no. 9, pp. 2407–2423, Sep. 2004.

[3] H. L. Van Trees, *Optimal Array Processing (Detection, Estimation, and Modulation Theory, Part IV)*. New York: Wiley-Interscience, 2002.

[4] K. L. Bell, Y. Ephraim, and H. L. V. Trees, "A Bayesian approach to robust adaptive beamforming," *IEEE Trans. Signal Process.*, vol. 48, no. 2, pp. 386–398, Feb. 2000.

[5] S. A. Vorobyov, A. B. Gershman, and Z.-Q. Luo, "Robust adaptive beamforming using worst case performance optimization," *IEEE Trans. Signal Process.*, vol. 51, no. 2, pp. 313–324, Feb. 2003.

[6] R. G. Lorenz and S. P. Boyd, "Robust minimum variance beamforming," *IEEE Trans. Signal Process.*, vol. 53, no. 5, pp. 1684–1696, May 2005.

[7] H. Cox, "Effects of random steering vector errors in the Applebaum array," *J. Acoust. Soc. Amer.*, vol. 54, pp. 771–785, Sep. 1973.

[8] A. Paulraj and T. Kailath, "Direction of arrival estimation by eigenstructure methods with imperfect spatial coherence of wave fronts," *J. Acoust. Soc. Amer.*, vol. 83, pp. 1034–1040, Mar. 1988.

[9] M. Wax and Y. Anu, "Performance analysis of the minimum variance beamformer in the presence of steering vector errors," *IEEE Trans. Signal Process.*, vol. 44, no. 4, pp. 938–947, Apr. 1996.

[10] L. Vandenberghe and S. Boyd, "Semidefinite programming," *SIAM Rev.*, vol. 38, no. 1, pp. 40–95, Mar. 1996.

[11] A. Beck and Y. C. Eldar, "Strong duality in nonconvex quadratic optimization with two quadratic constraints," *SIAM J. Optim.*, vol. 17, pp. 844–860, 2006.

[12] R. T. Rockafellar, *Convex Analysis*. Princeton, NJ: Princeton Univ. Press, 1970.

[13] Y. Ye and S. Zhang, "New results on quadratic minimization," *SIAM J. Optim.*, vol. 14, no. 1, pp. 245–267, 2003.

[14] C. Fortin and H. Wolkowicz, "The trust region subproblem and semidefinite programming," *Optim. Methods Softw.*, vol. 19, no. 1, pp. 41–67, 2004.

[15] J. J. Moré and D. C. Sorensen, "Computing a trust region step," *SIAM J. Sci. Statist. Comput.*, vol. 4, no. 3, pp. 553–572, 1983.

[16] A. L. Fradkov and V. A. Yakubovich, "The S-procedure and the duality relation in convex quadratic programming problems," *Vestnik Leningrad. Univ*, vol. 1, Mat. Meh. Astronom. Vyp. 1, pp. 81–87, 155, 1973.

[17] M. S. Bazaraa, H. D. Sherali, and C. M. Shetty, *Nonlinear Programming: Theory and Algorithms*, 2nd ed. New York: Wiley, 1993.

[18] A. Ben-Tal and A. Nemirovski, *Lectures on Modern Convex Optimization*, ser. MPS-SIAM Series on Optimization. Philadelphia, PA: SIAM, 2001.

[19] W. Gander, G. H. Golub, and U. von Matt, "A constrained eigenvalue problem," *Linear Algebra Appl.*, vol. 114-115, pp. 815–839, 1989.

[20] J. F. Sturm, "Using SeDuMi 1.02, a Matlab toolbox for optimization over symmetric cones," *Optim. Methods Softw.*, vol. 11-12, pp. 625–653, 1999.

Subspace Direction Finding With an Auxiliary-Vector Basis

Rohan Grover, *Student Member, IEEE*,
Dimitris A. Pados, *Member, IEEE*, and
Michael J. Medley, *Member, IEEE*

***Abstract*—We develop a new subspace direction-of-arrival (DOA) estimation procedure that utilizes a noneigenvector basis. Computation of the basis is carried out by a modified version of the orthogonal auxiliary-vector (AV) filtering algorithm. The procedure starts with the linear transformation of the array response scanning vector by the input autocorrelation matrix. Then, successive orthogonal maximum cross-correlation auxiliary vectors are calculated to form a basis for the scanner-extended signal subspace. As a performance evaluation example, our studies for uncorrelated sources demonstrate a gain in the order of 15 dB over MUSIC, 7 dB over ESPRIT, and 3 dB over the grid-search maximum likelihood DOA estimator at probability of resolution 0.9 with a ten-element array and reasonably small observation data records. Results for correlated sources are reported as well.**

***Index Terms*—Adaptive filtering, angle-of-arrival (AOA) estimation, auxiliary-vector (AV) algorithm, direction-of-arrival (DOA) estimation, small sample support, source localization.**

I. INTRODUCTION

Solutions for the classical direction-of-arrival (DOA) estimation problem can be broadly categorized into maximum-likelihood (ML)-type algorithms [1], which are based on techniques for the maximization of the probability density function of the received signal, and subspace algorithms, which are based on the decomposition of the autocovariance matrix of the received signal. Among the most successful and popular subspace algorithms are the MUSIC [2] and ESPRIT [3] procedures. In general, ML-type algorithms have superior performance compared to subspace-based techniques when the signal-to-noise ratio (SNR) is small or the number of snapshots is small. Also, the performance of subspace-based estimators degrades substantially in the case of correlated signal sources as compared to ML schemes.

In this correspondence, we attempt to exploit the structure of the received data autocovariance matrix in a new way. When K distinct signals in space impinge on M antenna elements ($K < M$), the input autocovariance matrix consists of a rank K signal subspace and a rank $M - K$ noise subspace. Using the concept of maximum cross-correlation auxiliary vectors (AVs) [4], we create a new *extended* noneigenvector signal subspace basis of rank $K + 1$ (eigendecomposition is not carried out at all). The *extended* signal subspace encompasses the *true* signal subspace of rank K and the scanning vector dimension itself. Then, the proposed DOA estimation algorithm simply looks for the collapse of the rank of the extended signal subspace from $K + 1$ to K when the scanning vector falls in the signal subspace. Extensive simulation studies demonstrate that significant resolution performance

Manuscript received March 16, 2005; revised September 9, 2005. The associate editor coordinating the review of this manuscript and approving it for publication was Prof. Yuri I. Abramovich. This work was supported in part by the National Science Foundation under Grant CCF-0219903 and the U.S. Air Force Office of Scientific Research under Grant FA9550-04-1-0256. This correspondence was presented in part at the SPIE Defense and Security Symposium, Orlando, FL, March 2005.

R. Grover and D. A. Pados are with the Department of Electrical Engineering, State University of New York at Buffalo, Buffalo, NY 14260 USA (e-mail: rgrover@eng.buffalo.edu; pados@eng.buffalo.edu).

M. J. Medley is with Air Force Research Laboratory, IFGC, Rome, NY 13441 USA (e-mail: michael.medley@rl.af.mil).

Digital Object Identifier 10.1109/TSP.2006.885771

1053-587X/$25.00 © 2006 IEEE